

**Supplemental information**

**Airway T cells are a correlate of**

**i.v. Bacille Calmette-Guerin-mediated protection  
against tuberculosis in rhesus macaques**

**Patricia A. Darrah, Joseph J. Zeppa, Chuangqi Wang, Edward B. Irvine, Allison N. Bucsan, Mark A. Rodgers, Supriya Pokkali, Joshua A. Hackney, Megha Kamath, Alexander G. White, H. Jacob Borish, L. James Frye, Jaime Tomko, Kara Kracinovsky, Philana Ling Lin, Edwin Klein, Charles A. Scanga, Galit Alter, Sarah M. Fortune, Douglas A. Lauffenburger, JoAnne L. Flynn, Robert A. Seder, Pauline Maiello, and Mario Roederer**

## Figure S1

A

	Current IV BCG Dose Ranging Study								Historical IV BCG Study	
Binned BCG dose ( $\log_{10}$ CFU)	Unvax	4.5 – 5.0	5.0 – 5.5		5.5 – 6.0		6.0 – 6.5	6.5 – 7.0	7.0 – 7.5	> 7.5
N (per binned dose group)	1	3	11		4		6	6	4	10
Actual BCG dose (CFU)	0	$3.9 \times 10^4$	$1.4 \times 10^5$	$2.0 \times 10^5$	$3.1 \times 10^5$	$4.2 \times 10^5$	$4.6 \times 10^5$	$2.5 \times 10^6$	$7.0 \times 10^6$	$2.5 \times 10^7$
N (per actual dose)	1	3	3	3	5	1	3	6	6	4
Vaccination cohort	b	a	b	a	b	b	a	a	a	H

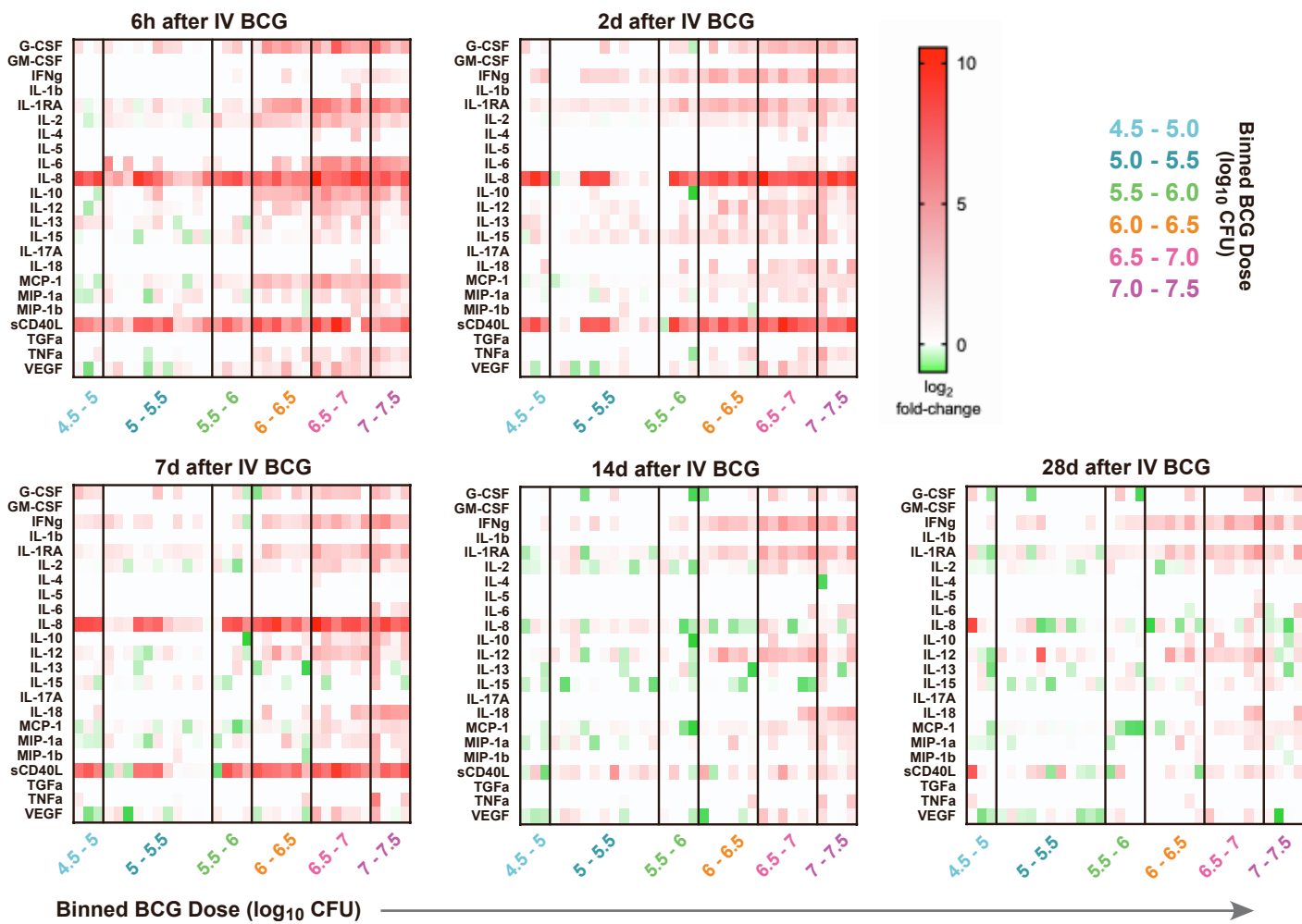
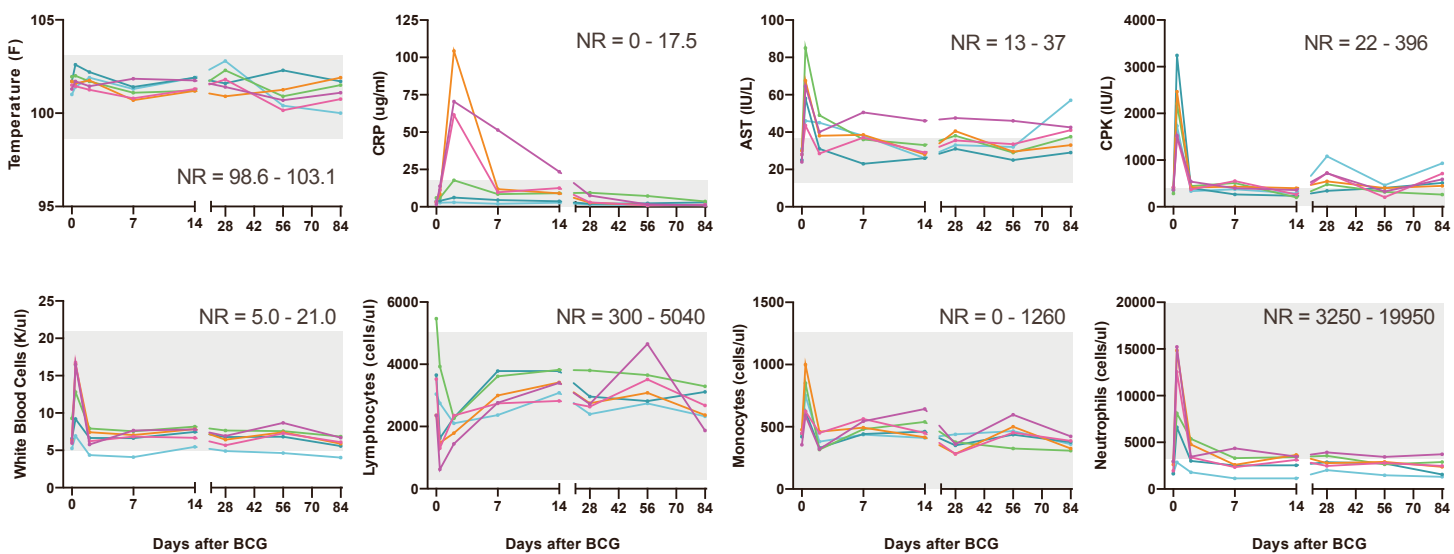
B

**Figure S1. Experimental design and timeline, related to all figures.**

**(A)** 34 rhesus macaques across two cohorts (a, b) were vaccinated with IV BCG at half-log increasing doses between 4.5 and 7.5 ( $\log_{10}$ ) CFU. 1 animal (cohort b) remained unvaccinated and served as an infection control. Actual (plated) doses of BCG administered and number of animals per actual dose and half-log binned dose group are noted. Data from a historical (H) IV BCG study (Darrah et al., 2020) are used in some analyses (**Figure S12**).

**(B)** PBMC and BAL were collected before (Pre) and at 2, 4, 8, and 12 weeks after BCG vaccination. Additionally, PBMC were collected at the time of Mtb challenge (week 24) as well as at 4-, 8-, and 12-weeks post-challenge. Animals were challenged 24 weeks after IV BCG vaccination with barcoded Mtb Erdman (4 to 17 CFU) via bronchoscope and were monitored for disease using longitudinal PET CT imaging and PBMC ELISpot, as well as pathological assessment and bacterial quantification at necropsy 12 weeks post-challenge (36 weeks after IV BCG).

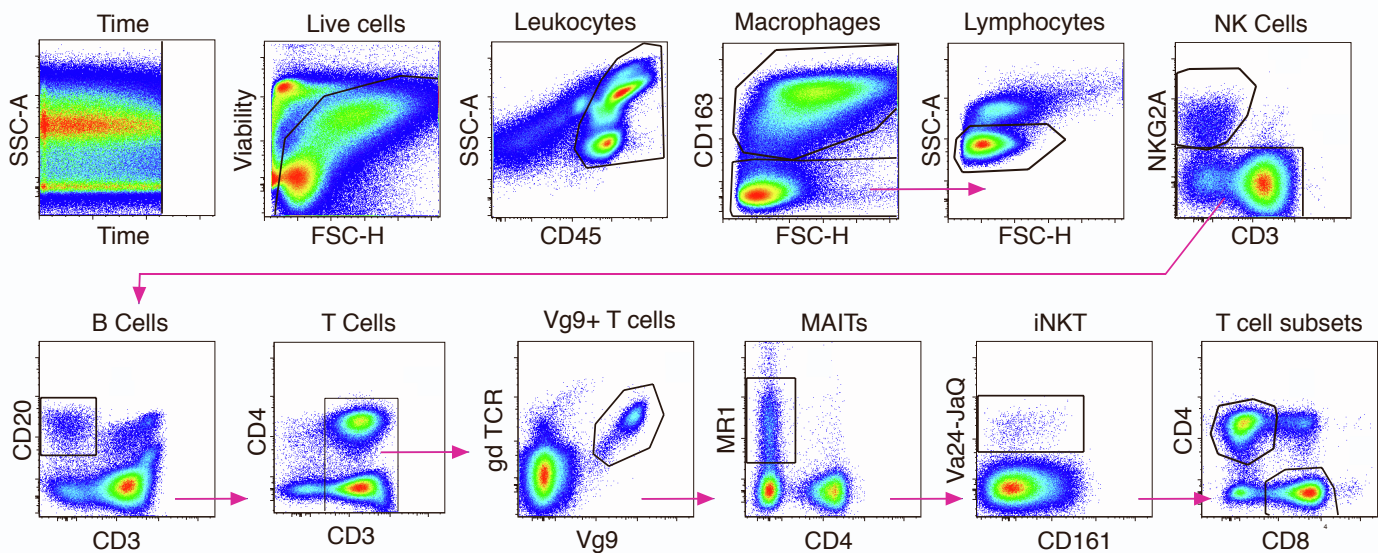
# Figure S2

**A**

**B**


**Figure S2. Systemic cytokine production and clinical parameters after IV BCG vaccination, related to Figure 1.**

**(A)** Cytokines (rows) were measured in the plasma before and after IV BCG vaccination using a 23-plex Luminex assay. Data are shown as  $\log_2$  fold changes over pre-vaccination for each macaque (columns, grouped by binned IV BCG dose) at 6 hours, 2 days, 7 days, 14 days, and 28 days after IV BCG vaccination.

**(B)** Macaques were monitored for changes in clinical parameters at various time points before and after IV BCG vaccination: temperature; C-reactive protein (CRP) as a marker of inflammation; Liver function (AST); muscle damage (CPK); White blood cells; lymphocytes; monocytes; neutrophils. Data are shown as median values for each dose group. Normal ranges (NR) for rhesus macaques are listed and depicted by shaded area.

**Figure S3**

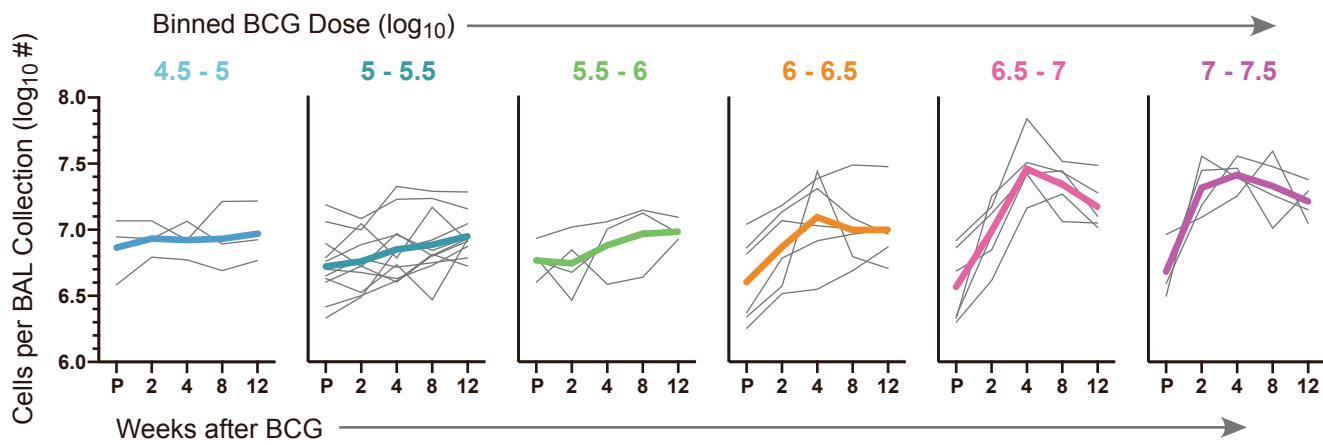
Marker	Clone	Company	Fluorochrome
LIVE/DEAD	Fixable Blue Dead Cell Stain	ThermoFisher Scientific	(U450)
CD45	D058-1283	BD Biosciences	BV510
CD3	SP34-2	BD Biosciences	BV650
CD4	SK3	BD Biosciences	BUV737
CD8	RPA-T8	BD Biosciences	BUV395
TCR $\gamma\delta$	5A6.E9	ThermoFisher Scientific	PE
TCR V $\gamma$ 9	7A5	ThermoFisher Scientific	Alexa Fluor 680
MR1 tetramer	Rh/5-OP-RU	NIH Tetramer Core	BV421
V $\alpha$ 24-J $\alpha$ Q	6b11	BD Biosciences	BV711
CD69	TP1.55.3	Beckman Coulter	ECD
NKG2A	Z199	Beckman Coulter	APC
HLA-DR	TU36	ThermoFisher Scientific	PE-Cy5.5
CD20	2H7	BioLegend	BV570
CD11b	HP-3G10	BioLegend	BV605
CD163	GHI/61	BioLegend	APC-Cy7
CD14	M5E2	BioLegend	BV785
CD16	3G8	BD Biosciences	BUV496
CD66abce	TET2	Miltenyi Biotec	FITC
CD11c	3.9	BioLegend	PE-Cy7
CD123	6H6	BioLegend	PE-Cy5

**Figure S3. Flow cytometry panel for characterization of leukocytes in rhesus BAL, related to Figure 1.**

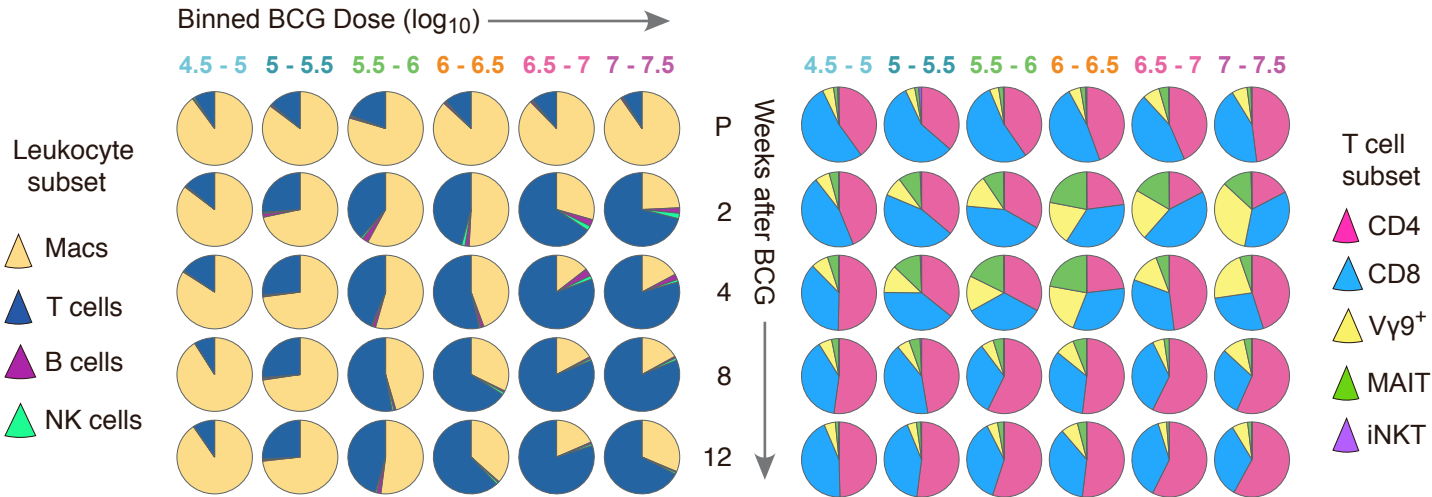
BAL samples were stained for flow cytometry fresh and without stimulation. For each surface marker included in the panel, the antibody clone, source, and fluorochrome are listed. Events were gated by time followed by live leukocyte (CD45+) detection. Macrophages were gated using CD163 and lymphocytes were gated for NK cells (CD3-NKG2A+), B cells (CD3-CD20+) and then total T cells. T cell subsets included V $\gamma$ 9+  $\gamma$  $\delta$  T cells, MR1-tetramer+ MAIT cells, V $\alpha$ 24-J $\alpha$ Q+ iNKT cells, and conventional CD4 and CD8 T cells.

# Figure S4

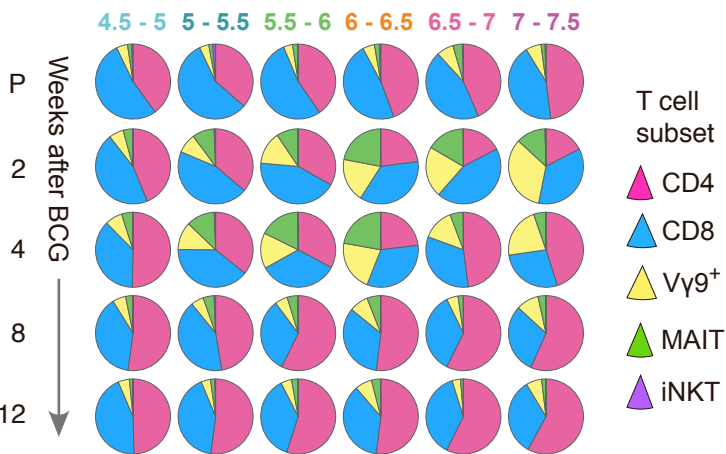
## A. BAL



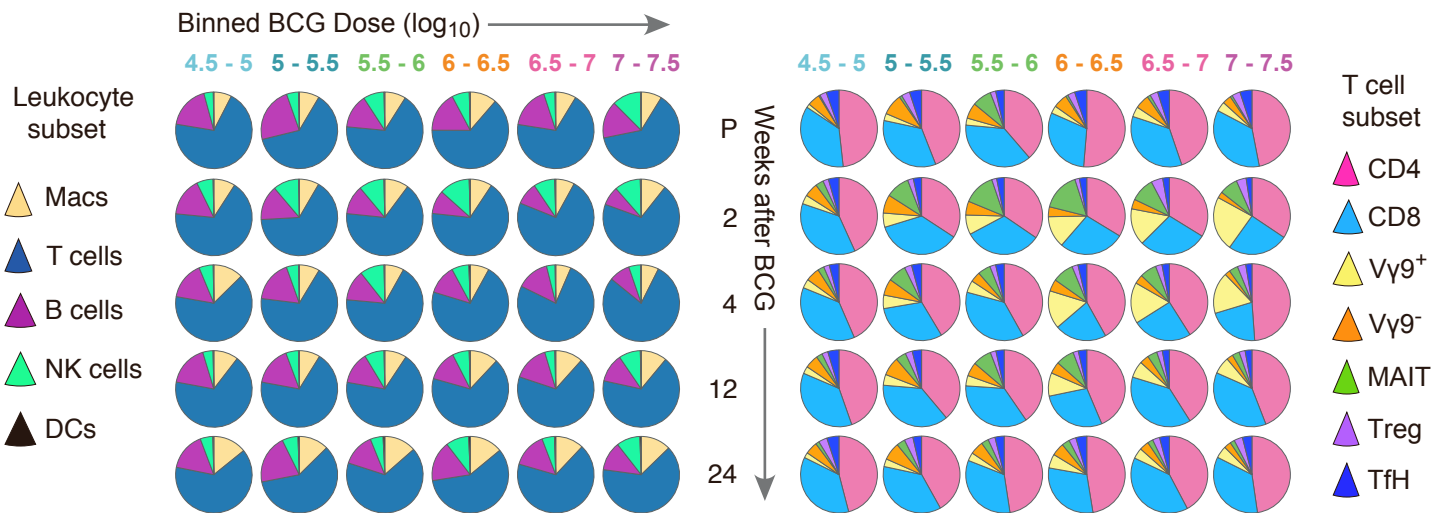
## B. BAL



## C. BAL



## D. PBMC



## E. PBMC

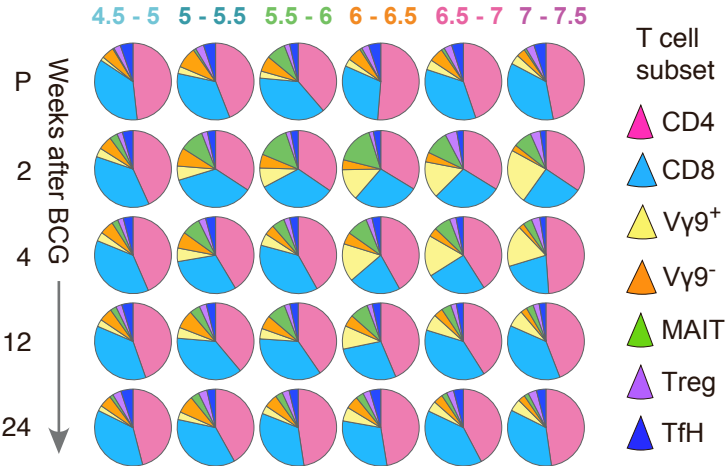


**Figure S4. Serial assessment of leukocyte composition in BAL or blood after IV BCG vaccination, related to Figure 1.**

**(A)** Number ( $\log_{10}$ ) of total live leukocytes per BAL collection before (Pre; P) and at 2, 4, 8, and 12 weeks after IV BCG vaccination as determined by acridine orange/propidium iodide (AO/PI) staining. Shown are data from individual macaques (thin grey lines) and medians (thick colored lines) for each BCG binned dose group.

**(B)** The average proportion of macrophages, T cells, B cells and NK cells within total live leukocytes in BAL as identified by flow cytometry (**Figure S3**) for each dose group (columns) over time (rows).

**(C)** Proportion of live CD3+ T cells classified as CD4 T cells, CD8 T cells, V $\gamma$ 9+  $\gamma$  $\delta$  cells, MR1+ MAIT cells, and Vo24+ iNKT cells in BAL as identified by flow cytometry (**Figure S3**).

**(D)** The average proportion of macrophages, T cells, B cells, NK cells and dendritic cells within total live leukocytes in PBMC as identified by flow cytometry (**Figure S5**) for each dose group (columns) before and up to 24 weeks after BCG (rows).

**(E)** Proportion of live CD3+ T cells classified as CD4 T cells, CD8 T cells,  $\gamma$  $\delta$  T cells (V $\gamma$ 9+ or V $\gamma$ 9-), MR1 tetramer+ MAIT cells, CD25+CD127- regulatory T cells (Treg), or CXCR5+ICOS+PD-1+ follicular helper T cells (Tfh) in PBMC as identified by flow cytometry (**Figure S5**).

Figure S5

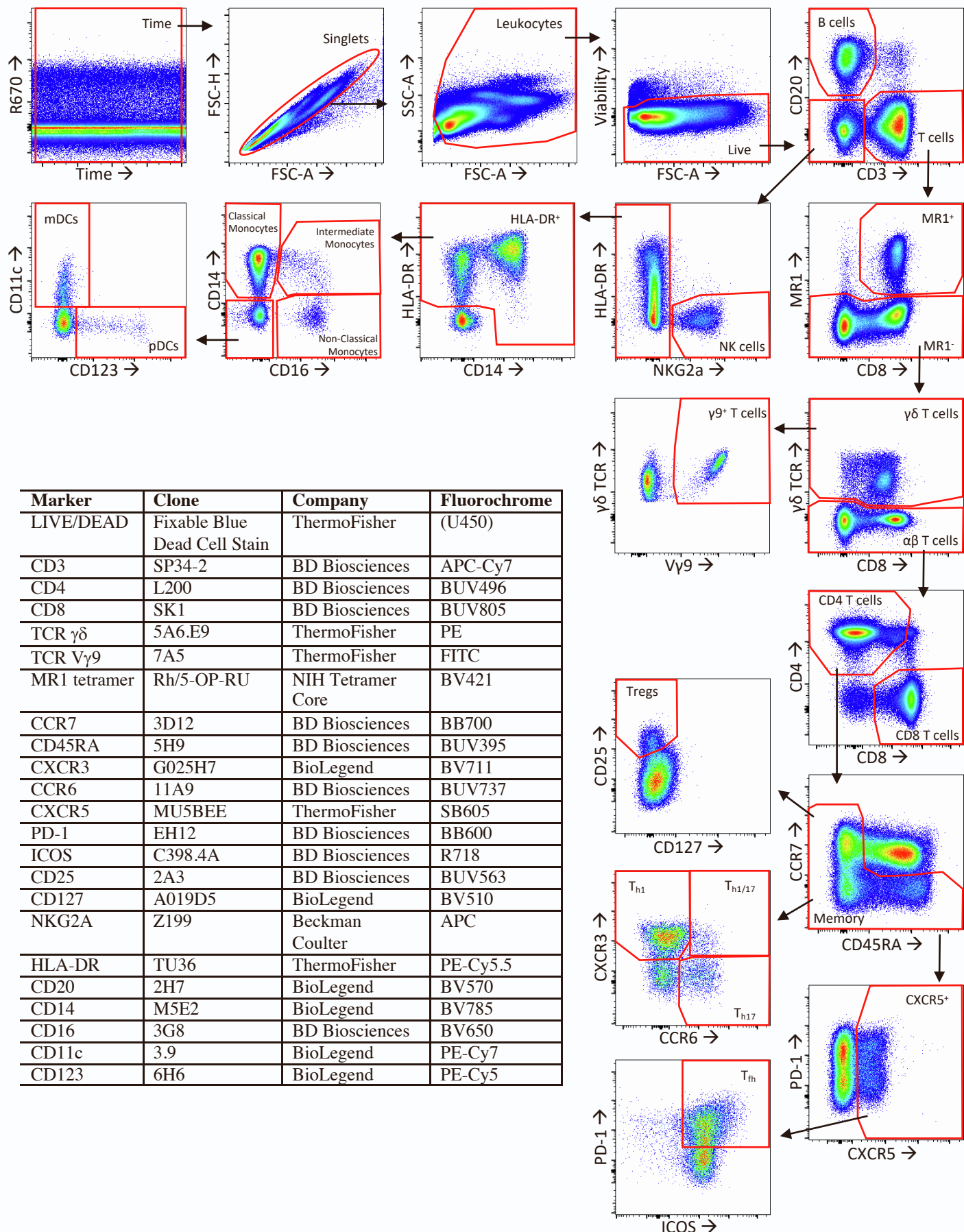
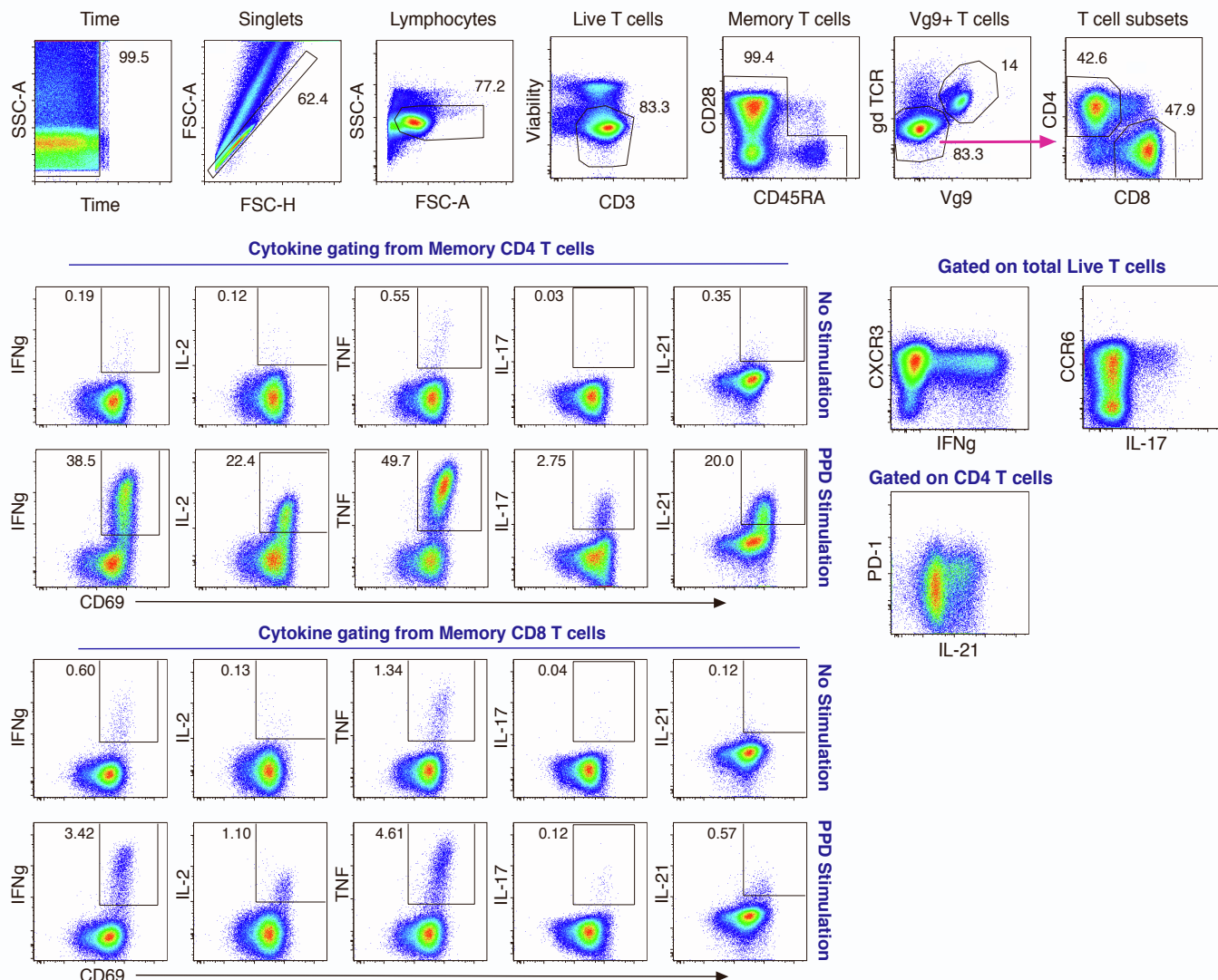


**Figure S5. Flow cytometry panel for characterization of leukocytes in rhesus PBMC, related to Figure 1.**

Cryopreserved PBMC samples were thawed and stained for flow cytometry without stimulation. For each surface marker included in the panel, the antibody clone, source, and fluorochrome are listed. Events were gated by time and then for singlets. Live cells were gated for B cells (CD20+), T cells (CD3+), or non-B/non-T cells. CD20-CD3- cells were gated for NK cells (NKG2A+HLA-DR-); HLA-DR+ cells were divided into monocyte subsets (based on CD14 and CD16) or dendritic cell subsets (based on CD11c or CD123). CD3+ T cells were gated for MR1 tetramer+ CD8+ MAIT cells, V $\gamma$ 9+  $\gamma$  $\delta$  T cells, or CD4+ and CD8+ T cells. Following total memory selection of CD4 T cells (based on CCR7 and CD45RA), regulatory T cells (T regs) were gated as CD25+CD127 $^{low}$  and T follicular helper cells were gated as CXCR5+PD1+ICOS+. The expression of chemokine receptors associated with Th1 (CXCR3) or Th17 (CCR6) is shown for total memory CD4 T cells.

**Figure S6**



Marker	Clone	Company	Fluorochrome
Live/Dead	Fixable Blue Dead Cell Stain	ThermoFisher Scientific	(U450)
CD4	S3.5	ThermoFisher Scientific	PE-Cy5.5
CD8	SK1	BD Biosciences	BUV805
Pan $\gamma\delta$ TCR	5A6.E9	ThermoFisher Scientific	PE
TCR V $\gamma$ 9	7A5	ThermoFisher Scientific	Alexa Fluor 680
CD28	CD28.2	BD Biosciences	PE-Cy5
CD45RA	L48	BD Biosciences	PE-Cy7
CXCR3	G025H7	BioLegend	BV711
CCR6	11A9	BD Biosciences	BUV737
PD-1	EH12	BD Biosciences	BV785
CD3	SP34-2	BD Biosciences	APC-Cy7
CD69	TP1.55.3	Beckman Coulter	ECD
IFN- $\gamma$	B27	BD Biosciences	APC
IL-2	MQ1-17H12	BD Biosciences	BV750
TNF	Mab11	BD Biosciences	BV650
IL-17A	BL168	BioLegend	BV570
IL-21	3A3N2.1	BD Biosciences	BV421

**Figure S6. Flow cytometry panel to measure antigen-specific T cells in BAL, related to Figure 1.**

BAL samples were stained for flow cytometry after *in vitro* stimulation with mycobacterial antigen. For each surface or intracellular (shaded) marker included in the panel, the antibody clone, source, and fluorochrome are listed. Events were gated by time and then for singlets and lymphocytes (based on forward and side scatter). Live CD3+ T cells were gated for total memory T cells using CD28 and CD45RA. After gating V $\gamma$ 9+  $\gamma$  $\delta$  T cells, CD4 and CD8 T cells were gated. Cytokine staining (IFN $\gamma$ , IL-2, TNF, IL-17, or IL-21 against CD69) in CD4 and CD8 T cells is shown for a representative unstimulated and PPD stimulated BAL sample. The expression of CXCR3, CCR6, and PD-1 on T cells is also shown for the same stimulated sample.

# Figure S7

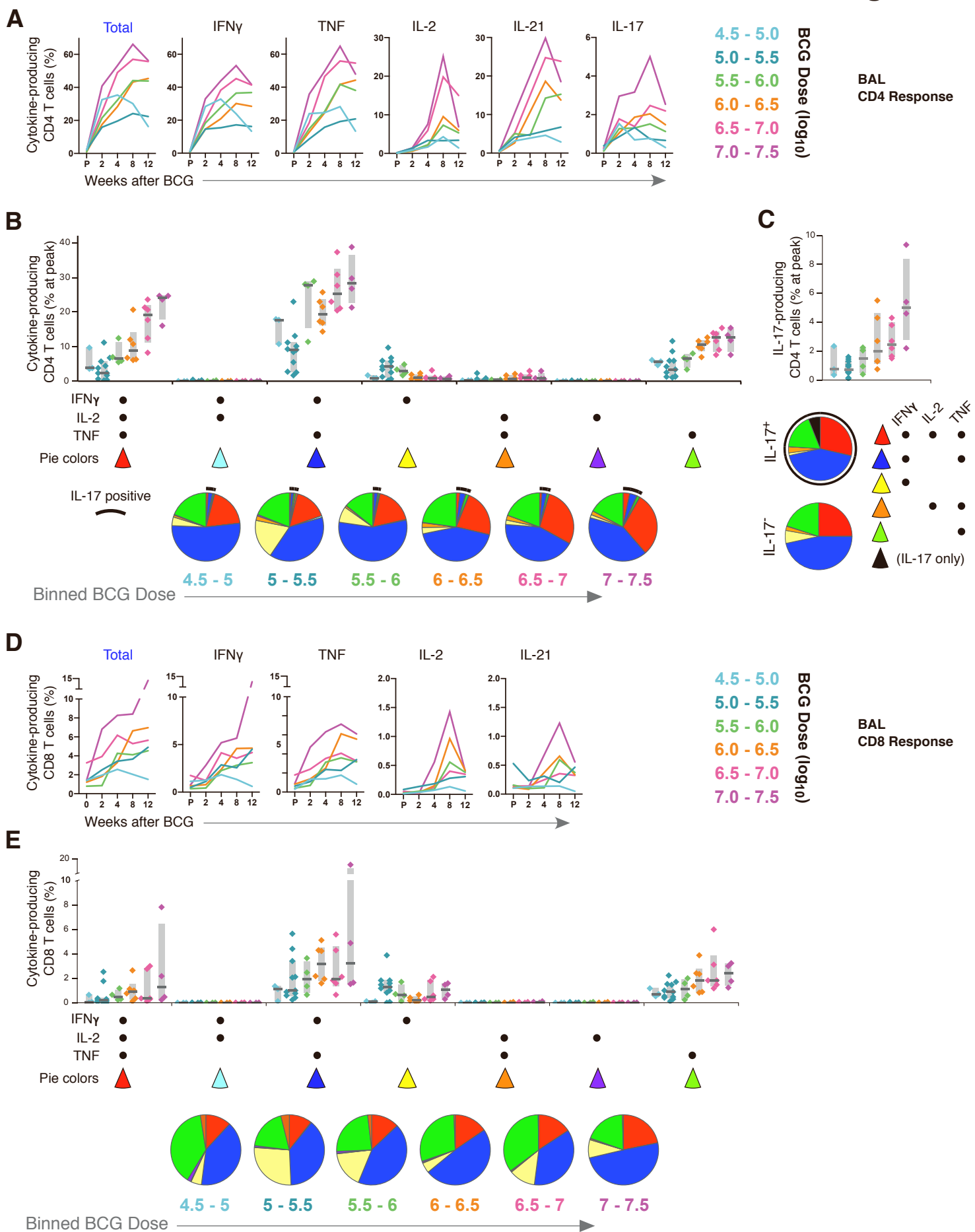


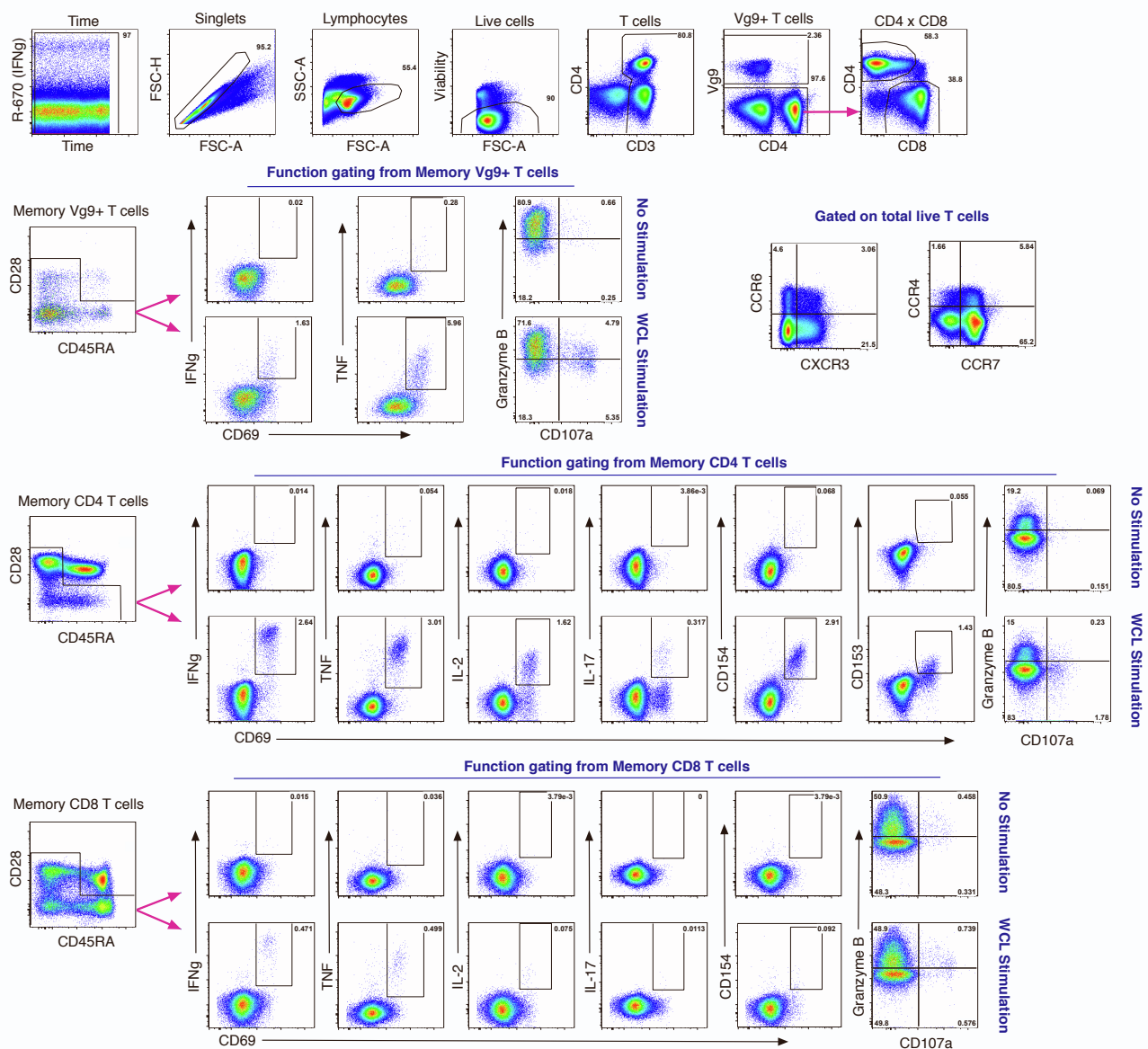
**Figure S7. Composition of T cell cytokine responses in BAL after IV BCG immunization, related to Figure 1.**

**(A, D)** Frequencies of memory CD4 **(A)** or CD8 **(D)** T cells in BAL producing IFN $\gamma$ , TNF, IL-2, IL-21, or IL-17 (any combination (Total), or individual) following *in vitro* stimulation with mycobacterial antigens (WCL) and identified by flow cytometry (**Figure S6**); shown are median responses for each binned dose group before (Pre, P) or 2, 4, 8, and 12 weeks after IV BCG.

**(B, E)** Peak (8 weeks) antigen-specific CD4 **(B)** and CD8 **(E)** T cell responses were further characterized as the frequency (bar graphs) or proportion (pie graphs) of cells producing every combination of IFN $\gamma$ , IL-2, or TNF. Frequencies from individual macaques are shown with interquartile range (shaded) and median (horizontal bar). Pie graphs of peak CD4 responses in **(B)** indicate the proportions of IFN $\gamma$ , IL-2, and TNF production without or with IL-17 production (black pie arcs).

**(C)** Peak (8 weeks) frequency of IL-17 producing memory CD4 T cells (bar graphs) and the proportions (pie graphs) of IFN $\gamma$ , IL-2, and TNF production within IL-17-positive (black arc) and IL-17-negative CD4 T cells for all (averaged) dose groups; black pie slice indicates IL-17 single-positive cells.

Figure S8



Marker	Clone	Company	Fluorochrome
LIVE/DEAD	Fixable Blue Dead Cell Stain	ThermoFisher Scientific	(U450)
CD4	L200	BD Biosciences	BUV496
CD8	SK1	BD Biosciences	BUV805
TCR V $\gamma$ 9	7A5	ThermoFisher Scientific	FITC
CD28	CD28.2	BD Biosciences	PE-Cy5
CCR7	150503	BD Biosciences	Alexa Fluor 700
CD45RA	L48	BD Biosciences	PE-Cy7
CD28	CD28.2	BD Biosciences	PE-Cy5
CXCR3	G025H7	BioLegend	BV605
CCR6	11A9	BD Biosciences	BUV737
CCR4	L291H4	BioLegend	BV510
PD-1	EH12	BD Biosciences	BUV395
CD107a	H4A3	BD Biosciences	BUV395
CD3	SP34-2	BD Biosciences	APC-Cy7
CD69	TP1.55.3	Beckman Coulter	ECD
IFN- $\gamma$	B27	BD Biosciences	APC
IL-2	MQ1-17H12	BD Biosciences	BV750
TNF	Mab11	BD Biosciences	BV650
IL-17A	BL168	BioLegend	BV570
Granzyme B	GRB18	ThermoFisher Scientific	PE-Cy5.5
CD153	116614	R&D Systems	PE
CD154	TRAP1	BD Biosciences	BV421

**Figure S8. Flow cytometry panel to measure antigen-specific T cells in PBMC, related to Figure 2.**

Cryopreserved PBMC samples were batch-analyzed by flow cytometry after *in vitro* stimulation with mycobacterial antigen. For each surface or intracellular (shaded) marker included in the panel, the antibody clone, source, and fluorochrome are listed. Shown is cytokine production from a representative PBMC sample, with or without WCL stimulation. Events were gated by time and then for singlets and lymphocytes (based on forward and side scatter). Viable lymphocytes were gated for total CD3+ T cells and then gated for V $\gamma$ 9+  $\gamma$  $\delta$  T cells, CD4 and CD8 T cells. For each T cell subset, memory T cells were selected using CD28 and CD45RA. Depending on production by the individual subset, T cells were gated for production of IFN $\gamma$ , TNF, IL-2, IL-17, CD154, or CD153 against the activation marker CD69. Granzyme B and CD107 gates were drawn on total T cells but applied only to antigen-specific T cells. Expression of chemokine receptors (CXCR3, CCR6, CCR4, and CCR7) is shown for total T cells.

## Figure S9

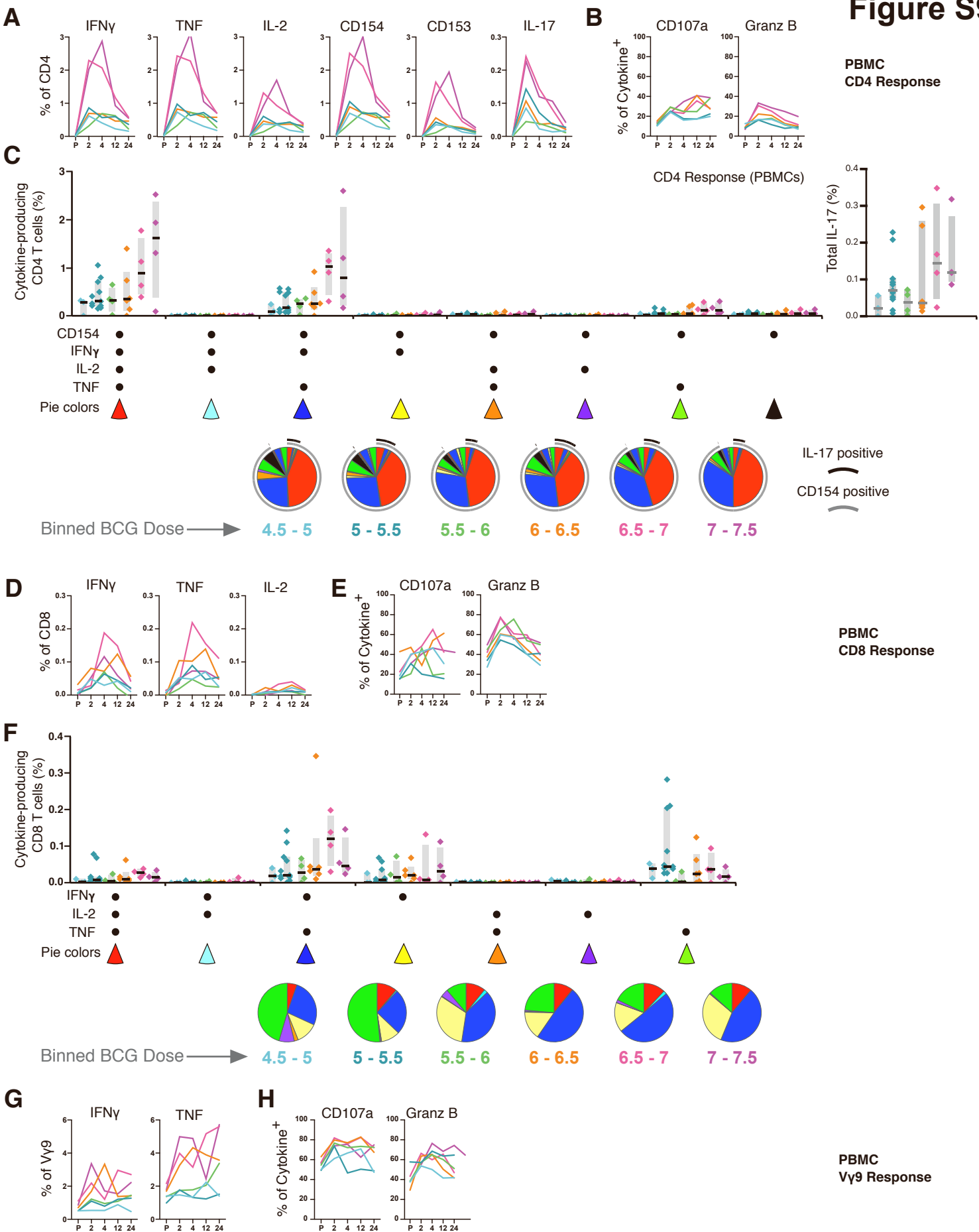


**Figure S9. Composition of T cell cytokine response in PBMC after IV BCG immunization, related to Figure 2.**

**(A, D, G)** Frequency of memory CD4 (A), CD8 (D), or V $\gamma$ 9+  $\gamma$  $\delta$  (G) T cells in PBMC producing IFN $\gamma$ , TNF, IL-2, CD154, CD153, or IL-17 following *in vitro* stimulation with mycobacterial antigens (WCL) as identified by flow cytometry (Figure S8). Shown are median responses for each IV BCG dose group before (Pre, P) and 2, 4, 12, and 24 weeks after BCG immunization.

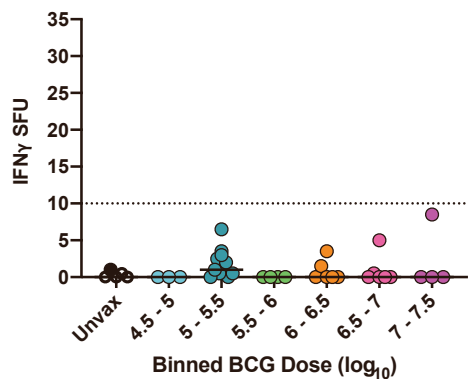
**(B, E, H)** Percent of mycobacterial-responsive (cytokine-producing) CD4 (B), CD8 (E), or V $\gamma$ 9+  $\gamma$  $\delta$  (H) T cells expressing CD107a or granzyme B.

**(C, F)** The composition of the total T cell response captured for each BCG dose group was characterized as the relative proportion of antigen-stimulated cells producing every combination of CD154, IFN $\gamma$ , IL-2, and TNF, with or without IL-17 (CD4, C) or any combination of IFN $\gamma$ , IL-2, and TNF (CD8, F). Bar graphs show the frequency of memory CD4 or CD8 T cells in PBMC producing cytokines in response to WCL at the peak of the immune response (4 weeks). Responses from individual macaques (symbols) are shown with interquartile range (bar) and median (horizontal line). Pie graphs represent the average proportion of total cytokine production at peak comprising each cytokine combination for each IV BCG dose group; the proportion of the total response producing IL-17 at peak (C, right) is indicated with a black arc (pies) for CD4 T cells only.

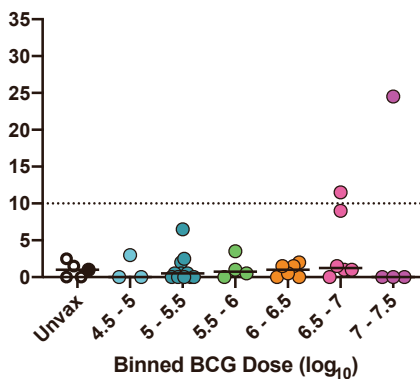
# Figure S10

**A**

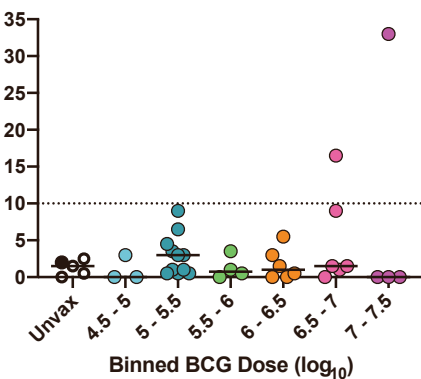
### ESAT-6 Pre-Mtb



### CFP-10 Pre-Mtb



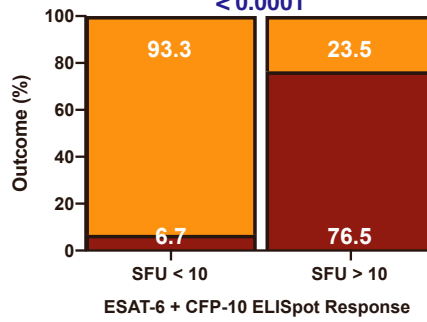
### ESAT-6 + CFP-10 Pre-Mtb



**B**

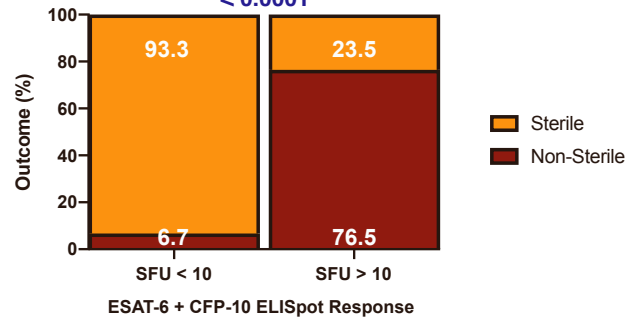
### Lung Sterility

$< 0.0001$



### Lung Lymph Node Sterility

$< 0.0001$



**C**

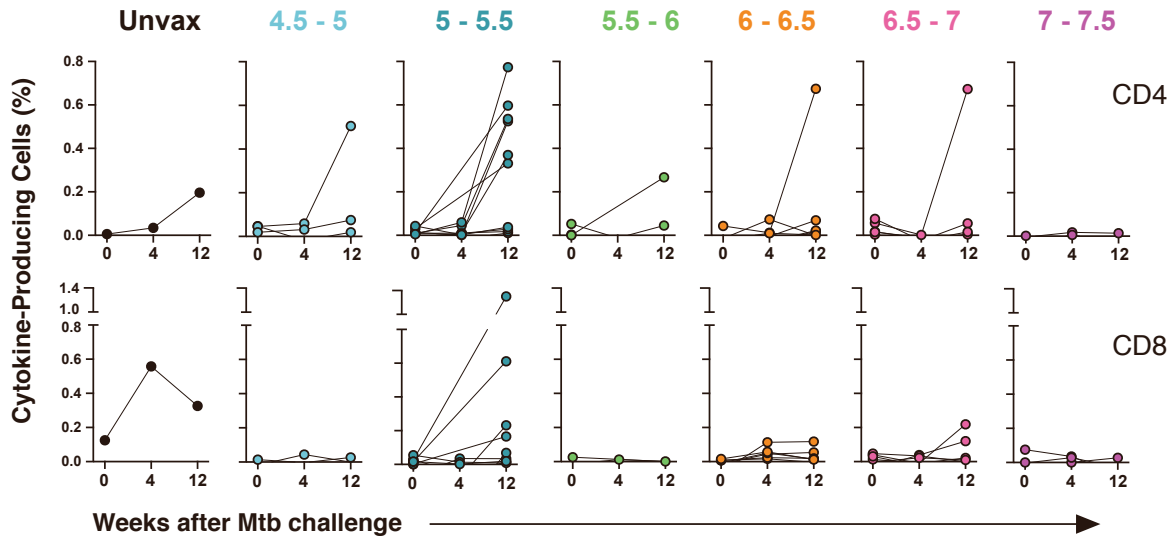


**Figure S10. Mtb-specific responses prior to and after Mtb infection in IV BCG vaccinated macaques, related to Figure 5.**

**(A)** Pre-challenge PBMC responses against antigens found in Mtb (but not BCG), ESAT-6, CFP-10, or ESAT-6 + CFP-10 peptides combined, as determined by IFN $\gamma$  ELISpot. Symbols represent individual animals; horizontal solid bars represent the median; dashed horizontal line represents the SFU cut-off at which at least 95% of uninfected animals fall for each antigen.

**(B)** Outcome (%) of macaques with sterile or non-sterile lung or lung lymph nodes (i.e., 0 Mtb CFU) that are either positive ( $> 10$  SFU) or negative ( $< 10$  SFU) by ESAT-6 + CFP-10-responsive IFN $\gamma$  ELISpots. Fisher's exact test p-value reported (two-sided).

**(C)** Frequency of memory CD4 (top) or CD8 (bottom) T cells producing IFN $\gamma$ , IL-2, TNF, or IL-17 in response to ESAT-6 + CFP-10 peptides for individual animals in each binned dose group at 0-, 4-, and 12-weeks post Mtb-challenge as measured by flow cytometry.

# Figure S11

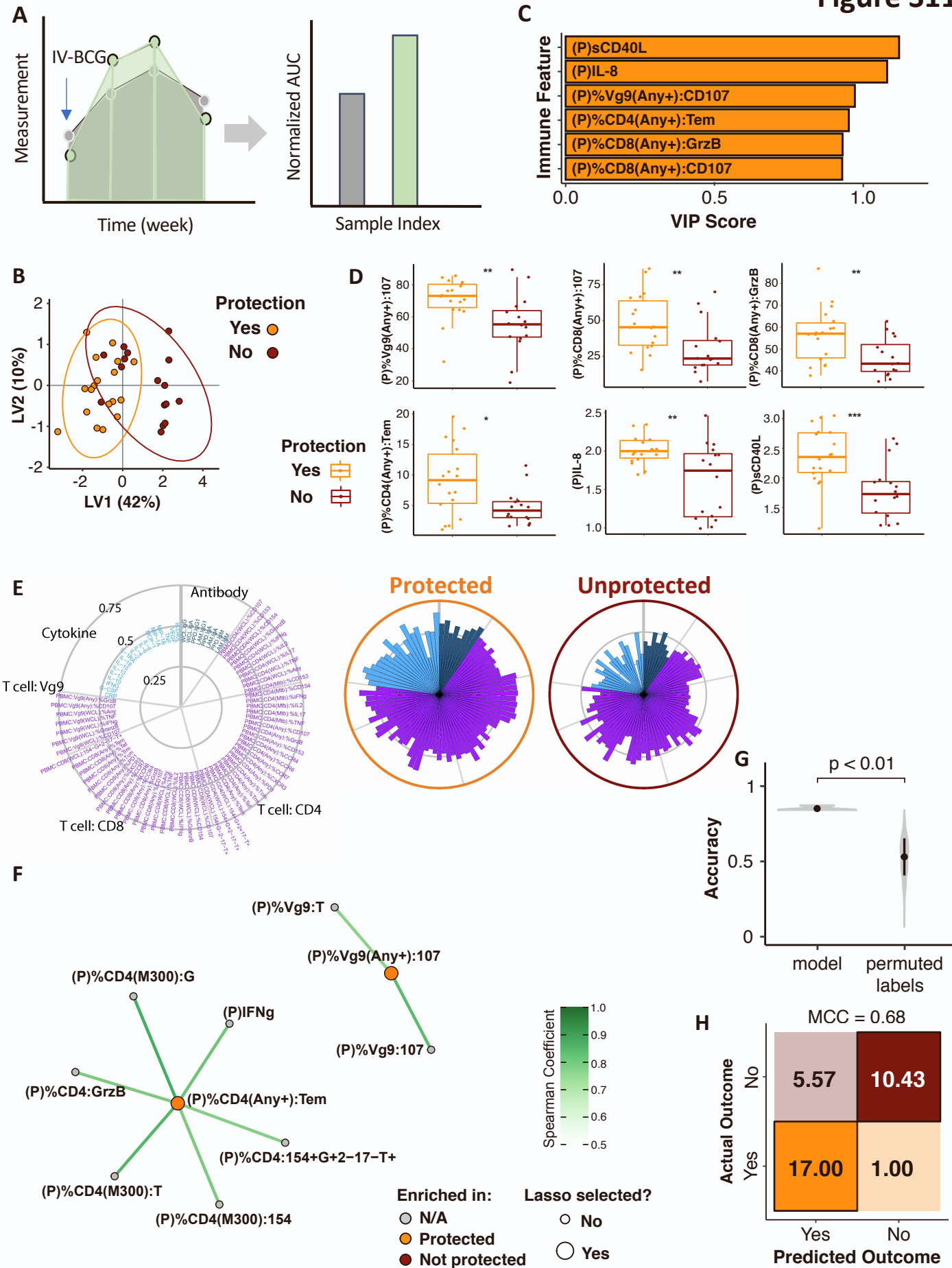


**Figure S11. Selected immune features from blood distinguish protected and unprotected macaques, related to Figure 6.**

**(A)** The schematic plot shows the AUC calculation using the temporal profile of each immune measurement.

**(B–D)** The PLSDA scores plot shows the degree of discrimination of protection achievable following the LASSO selection of immune features from blood **(B)**. Each symbol is one animal, and ellipses indicate 95% confidence regions assuming a multivariate  $t$  distribution. **(C)** The bar plot shows the Variable Importance in Projection (VIP) score of the six selected features required to separate the groups (P, PBMC or plasma); the magnitude indicates the importance of the features to group separation and the color of the bar indicates in which group the feature is enriched (higher median value). **(D)** Univariate box plot shows the distribution of each selected feature. Each box represents the IQR (box) with median (bar) and whiskers ( $1.5 * \text{IQR}$ ). \*  $p < 0.05$ , \*\*  $p < 0.01$ , \*\*\*  $p < 0.001$ , \*\*\*\*  $p < 0.0001$ .

**(E)** Polar plots depict the mean percentile of each measurement across the protected and unprotected groups. The major slices represent the antibody measurements, numbers of different cell types, and numbers or frequencies of T cells with different expressed cytokine expressions. The length of the wedge depicts the mean percentile ranging from 0–0.75 with a step of 0.25.

**(F)** The correlation network shows the co-correlated features (small grey nodes) that are significantly correlated ( $p < 0.05$  after multiple test correction using the Benjamini-Hochberg procedure, Spearman's correlation  $> 0.7$ ) with the model selected features (large nodes, colored by the protection group in which they are enriched.) See also **Table S3**.

**(G–H)** The performance and robustness of the model are validated with permutation testing and confusion matrix. The violin plot shows the distributions of repeated classification accuracy testing using label permutation; the p-value is two-sided **(G)**. Black squares indicate the median accuracy and black lines represent one SD. **H)** Average confusion matrix of our PLSDA model. The stratified five-fold cross-validation strategy was applied to the PLSDA model 100 times, Matthews correlation coefficient (MCC).

## Figure S12

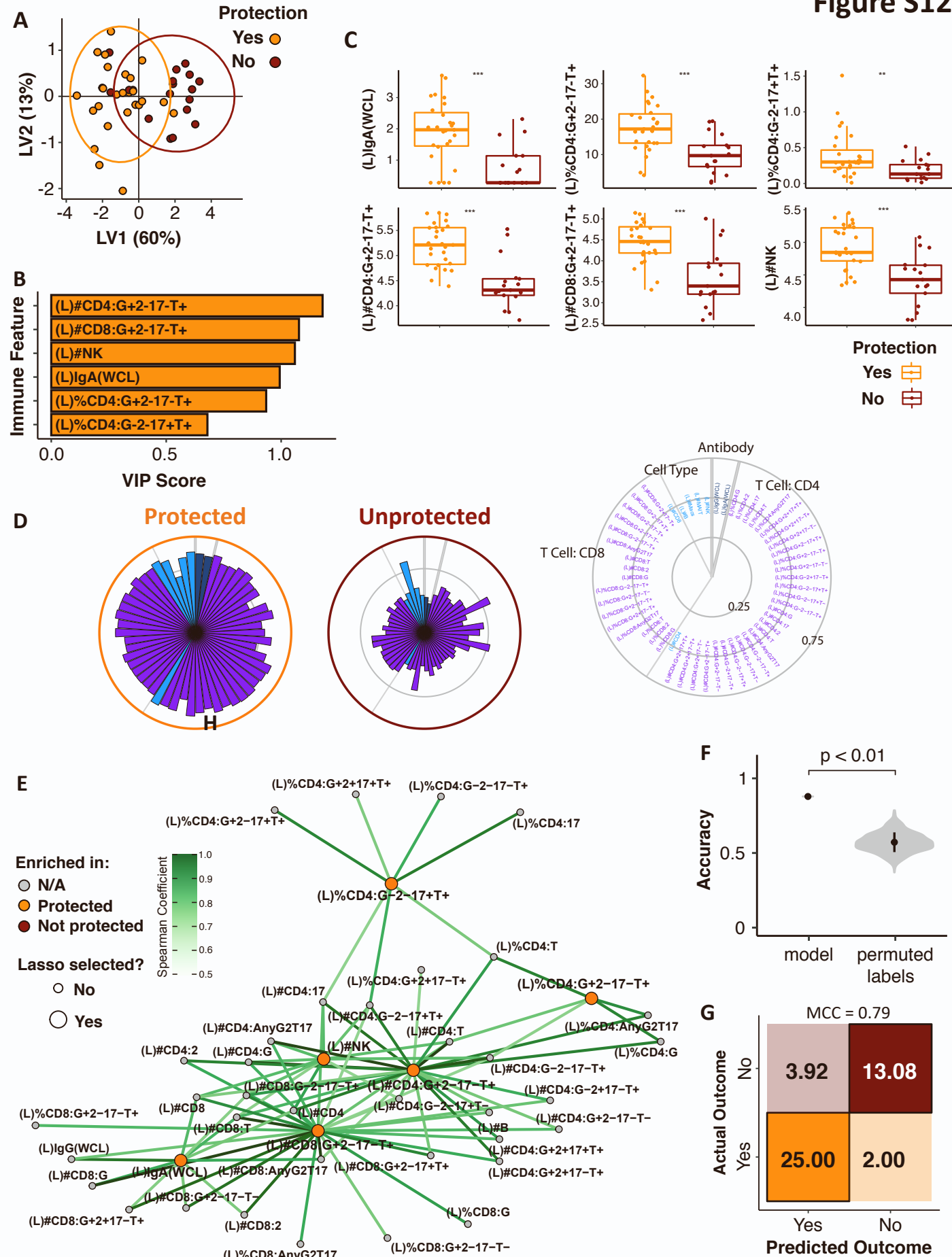


**Figure S12. Selected features in BAL from current and historical cohort distinguish protected and unprotected macaques, related to Figure 6.**

**(A–C)** The PLSDA scores plot shows the degree of discrimination that is achievable across the groups following the LASSO feature selection. Each symbol is one sample, and ellipses indicate 95% confidence regions assuming a multivariate *t* distribution (A). The bar plot (B) shows the VIP score of the six selected features in BAL (L, lung) required to separate the groups; the magnitude indicates the importance of the features to group separation. The bar color indicates in which group the feature is enriched (higher median value). Univariate Box plots (C) show the distribution of each selected feature. Each box represents the IQR with median (central line) and whiskers (1.5 \* IQR). \*  $p < 0.05$ , \*\*  $p < 0.01$ , \*\*\*  $p < 0.001$ , \*\*\*\*  $p < 0.0001$ .

**(D)** Polar plots depict the mean percentile of each measurement across the protected and the unprotected groups. The major slices represent the antibody related measurements, cell type measurements and T cell measurements with different expressed cytokine expressions. The length of the wedge depicts the mean percentile ranging from 0–0.75 with the step of 0.25.

**(E)** The correlation network shows the co-correlated features (small grey nodes) that are significantly correlated ( $p < 0.05$  after Benjamini-Hochberg correction, Spearman's correlation  $> 0.7$ ) with the model selected features (large nodes colored by the protection group in which they are enriched). See also **Table S3**.

**(F)** The performance and robustness of the model are validated with permutation testing and confusion matrix. The violin plot shows the distributions of repeated classification accuracy testing using label permutation with two-sided *p*-value (F). Black squares indicate the median accuracy and black lines represent one SD. **(G)** Average confusion matrix of our PLSDA model. The stratified five-fold cross-validation strategy was applied to the PLSDA model 100 times; Matthews correlation coefficient (MCC).

**Table S2. Logistic Regression Analysis of Protection**

Predictor	$\beta$	SE $\beta$	Wald's $\chi^2$	<i>p</i>	Lower 95%	Upper 95%	Odds Ratio
Intercept	-4.0741	3.7536	1.1800	0.2778	-12.0539	3.2383	
IV BCG Dose ( $\log_{10}$ )	-0.5862	0.8347	0.4900	<b>0.4825</b>	-2.4194	0.9833	0.5564
<b>CD4 (% Ag-specific)</b>	0.2357	0.0908	6.7400	<b>0.0095</b>	0.0900	0.4563	<b>1.2659</b>
Overall model evaluation		<i>DF</i>	$\chi^2$	<i>p</i>			
Likelihood ratio test		2	20.8189	<b>&lt;.0001</b>			
Predictor	$\beta$	SE $\beta$	Wald's $\chi^2$	<i>p</i>	Lower 95%	Upper 95%	Odds Ratio
Intercept	-7.5460	3.2005	5.5600	0.0184	-14.5388	-1.7506	
<b>IV BCG Dose (<math>\log_{10}</math>)</b>	1.2869	0.5785	4.9500	<b>0.0261</b>	0.2393	2.5559	<b>3.6216</b>
<b>CD8 (% Ag-specific)</b>	-0.0040	0.1376	0.0000	<b>0.9771</b>	-0.2581	0.3000	0.9961
Overall model evaluation		<i>DF</i>	$\chi^2$	<i>p</i>			
Likelihood ratio test		2	7.8045	<b>0.0202</b>			
Predictor	$\beta$	SE $\beta$	Wald's $\chi^2$	<i>p</i>	Lower 95%	Upper 95%	Odds Ratio
Intercept	-18.4119	5.8343	9.9600	0.0016	-32.2591	-8.6427	
IV BCG Dose ( $\log_{10}$ )	-0.6791	0.8684	0.6100	<b>0.4342</b>	-2.5168	0.9816	0.5071
<b>CD4 (# Ag-specific <math>\log_{10}</math>)</b>	4.3572	1.6278	7.1600	<b>0.0074</b>	1.5570	8.1328	<b>78.0348</b>
Overall model evaluation		<i>DF</i>	$\chi^2$	<i>p</i>			
Likelihood ratio test		2	18.2412	<b>0.0001</b>			
Predictor	$\beta$	SE $\beta$	Wald's $\chi^2$	<i>p</i>	Lower 95%	Upper 95%	Odds Ratio
Intercept	-10.0320	3.8318	6.8500	0.0088	-18.7101	-3.3058	
IV BCG Dose ( $\log_{10}$ )	0.5955	0.7179	0.6900	<b>0.4068</b>	-0.8233	2.0601	1.8139
<b>CD8 (# Ag-specific <math>\log_{10}</math>)</b>	1.4740	1.1092	1.7700	<b>0.1839</b>	-0.5861	3.9090	4.3666
Overall model evaluation		<i>DF</i>	$\chi^2$	<i>p</i>			
Likelihood ratio test		2	9.7368	<b>0.0077</b>			

**Table S2. Logistic regression analysis of protection, related to Figures 1 and 5.**

Logistic regression analysis using peak frequencies and numbers of cytokine-producing memory CD4 and CD8 T cell frequencies and numbers from BAL, with IV BCG dose as fixed predictor variables. Each logistic regression model shows predictor name in first column with parameter estimate ( $\beta$ ), standard error of parameter estimate (SE  $\beta$ ), Wald Chi-Square test statistic (Wald  $\chi^2$ ), p-value for Wald test ( $p$ ), lower and upper 95% confidence interval bounds for parameter estimate, and an odds ratio. Each model was evaluated using a likelihood ratio test and degrees of freedom ( $DF$ ), Chi-Square test statistic ( $\chi^2$ ) and p-value for likelihood ratio test are reported. Predictor p-values are highlighted in bold text. If a p-value is statistically significant (less than 0.05), the corresponding odds ratio is highlighted in bold text.